Journal of Materials Chemistry

Cite this: J. Mater. Chem., 2012, 22, 14587

www.rsc.org/materials

PAPER

Novel sol–gel prepared zinc fluoride: synthesis, characterisation and acid–base sites analysis

Ying Guo,[a] Stefan Wuttke,[b] Alexandre Vimont,[c] Marco Daturi,[c] Jean-Claude Lavalley,[c] Katharina Teinz[a] and Erhard Kemnitz*[a]

Received 5th March 2012, Accepted 18th May 2012
DOI: 10.1039/c2jm31357j

The fluorolytic sol gel route sets a milestone in the development of synthesis methods for nanoscopic fluoride materials. They exhibit fundamentally distinct properties in comparison to classically prepared metal fluorides. To broaden this area, we report in this paper the first fluorolytic sol gel synthesis of ZnF_2. The obtained sol was studied with dynamic light scattering (DLS). The dried ZnF_2 xerogel was investigated with elemental analysis, thermal analysis, powder X ray diffraction (XRD), solid state MAS NMR, and N_2 adsorption desorption measurements. The characterisations revealed a remarkably high surface area of the sol gel prepared ZnF_2. To determine key parameters deciding its prospects in future catalytic applications, we studied the surface acidity basicity by using *in situ* FTIR with different probe molecules. Compared to the previously established MgF_2, weaker Lewis acid sites are predominant on the surface of ZnF_2 with some base sites, indicating its potential as a heterogeneous catalyst component. In short, we believe that the successful synthesis and detailed characterisation of nanoscopic ZnF_2 allow follow up work exploring its applications, and will lead to studies of more metal fluorides with similar methods.

Introduction

The fluorolytic sol gel synthesis has been recognised to be as powerful as the classic hydrolytic sol gel synthesis. Although this new approach for high surface area metal fluorides was devel oped just a few years ago, the already achieved results have given access to fundamental research insights and opened a very broad range of practical applications.[1,2] Since the early days of this approach, we have continuously worked on the fluorolytic sol gel synthesis of novel nanoscopic fluoride materials and on the evaluation of their properties. The latter is essential for a targeted application of the resulting fluorides in fields such as anti reflective coatings,[3] high performance ceramics[4] and heteroge neous catalysis.[5]

Compared to metal oxides, metal fluorides are distinguished by their much more pronounced surface acidity. Considering that heterogeneous acid catalysts are by far the most used cata lysts in the chemical industry,[6,7] acidic fluorides with high surface area can be very promising in this field either as an active component or as the support.[2] Indeed, as a heterogeneous catalyst, the sol gel prepared MgF_2 (and its variants) has revealed an extraordinary catalytic performance with high activity as well as high selectivity.[8–13] MgF_2 based catalysts are suitable for a very broad range of applications in these fields, which have been reviewed recently.[14]

Encouraged by the outstanding catalytic performances of MgF_2 based systems, we proposed to synthesise more nano scopic metal fluorides. We chose ZnF_2 as our primary research target due to the similarity between Zn and Mg. A comparison of the properties of Zn and Mg shows that they are comparable in many aspects including electron configuration, coordination number and ionic radius.[15] Because of the fully occupied d shell of Zn, the results are not surprising. Especially, ZnF_2 and MgF_2 are also identical in crystal structure, whereas other alkaline earth metal fluorides have different structures compared to MgF_2. In the screening for a substance comparable to MgF_2, we found that ZnF_2 is a favourable candidate.

Subsequently we aimed at a thorough investigation of the surface acid base properties of the ZnF_2, being aware of the importance of the knowledge for well directed catalytic appli cations and a systematic comparison with other fluorides. For instance, recently, the high selectivity of different sol gel prepared fluorides (AlF_3 and alkaline earth metal fluorides series) for the dehydrohalogenation of chlorofluoropropane derivatives has been associated with their acid base properties.[16] We have demonstrated the similarity of the MgF_2 and ZnF_2. Thus, based on the succesful investigation of MgF_2, we initiated a thorough acid base study of ZnF_2. Knowing the surface

[a]Institut fur Chemie, Humboldt Universitat zu Berlin, Brook Taylor Straße, D 124892, Berlin, Germany. E mail: erhard.kemnitz@chemie.hu berlin.de; Fax: +49 30 20937468; Tel: +49 30 20937555
[b]Department of Chemistry and Center for NanoScience (CeNS), University of Munich (LMU), Butenandtstraße 11, Munich, Germany
[c]Laboratoire Catalyse et Spectrochimie, UMR 6506, CNRS/ENSICAEN et Université de Caen Basse Normandie, Caen, France

properties of the catalyst is crucial for understanding the cata lytic reaction, which helps us in turn to improve the catalytic performance.

In light of this background, we report here for the first time the sol gel synthesis and characterisation of nanoscopic ZnF_2. To evaluate the robustness of this synthesis route, we performed the synthesis under both non aqueous and aqueous conditions respectively, which clarified the effects of water presence in the preparation process. The sol particle size distribution was determined with dynamic light scattering (DLS). Properties of the bulk material, *e.g.* the chemical composition, thermal behaviour and crystalline structure, were studied by various analytical approaches including elemental analysis, thermal analysis, powder X ray diffraction (XRD) and solid state MAS NMR. Surface area and textural information were determined by N_2 adsorption desorption measurements. Specifically, surface acid base sites were investigated by *in situ* FTIR spectroscopy of adsorbed probe molecules. To the best of our knowledge, no targeted acid base studies have been performed on a sol gel prepared zinc fluoride material so far. Our study explores the surface properties of the newly synthesised nanoscopic ZnF_2.

Experimental

Preparation of ZnF_2

HS ZnF_2 (*HS*: high surface) was synthesised under non aqueous conditions. $Zn(OOCCH_3)_2$ (Aldrich, 99.99%) was dehydrated at 70 °C *in vacuo* for 2 h before use. The obtained anhydrous $Zn(OOCCH_3)_2$ (1.78 g, 9.7 mmol) was dissolved in 100 ml water free methanol (dried over $Mg(OCH_3)_2$). A stoichiometric amount of methanolic HF solution (19.4 mmol) was added to the mixture. After ageing for 12 16 h at room temperature, the formed transparent sol was dried *in vacuo* and further calcined at 100 °C for 2 h.

The process of aqueous synthesis is similar to that of non aqueous synthesis, except that $Zn(OOCCH_3)_2$ and methanol were used as supplied. HF solution with various water contents was added at stoichiometric HF amounts. The obtained final products were labelled as ZnF_2 *n*, where *n* represents the HF concentration ($n = 100$, 71, or 40, indicating methanolic anhy drous HF, 71% HF or 40% HF aqueous solution, respectively).

Characterisation

The C and H contents were determined with a Leco CHNS 932 analyser. The F contents were determined with a fluoride sensi tive electrode. Before the analysis, the samples were digested by fusion with soda potash.

DLS measurements were taken with a Malvern Zetasizer Nano ZS in NIBS mode at 173°. The ZnF_2 sol sample was prepared in methanol (concentration = 0.2 mol L^{-1}) and filtered with a 450 nm nylon filter.

Thermal analysis experiments were performed by using the hyphenation of Netzsch STA 409C/CD and Balzers QMG 422 Quadrupol Mass spectrometry. Both DTA TG curves and the *m*/*z* ratio of the fragments were recorded during measurements.

XRD investigations were performed with a XRD 7 Seifert FPM diffractometer by using a CuKα beam. The anhydrous *HS* ZnF_2 sample was prepared in a glove box and protected with a polystyrene film.

The solid state MAS NMR spectra were collected with a Bruker Avance 400 Spectrometer using 2.5 mm MAS rotors. The resonance frequency for ^{19}F spectra was 376.4 MHz. The chemical shift of ^{19}F was calibrated with $CFCl_3$ as standard reference material.

N_2 adsorption desorption isotherms at 196 °C were measured with a Micromeritics ASAP 2020 instrument. The samples were first calcined at 200 °C for 2 h to remove adsorbed species and then degassed at 120 °C for 12 h. The specific surface area was calculated according to the BET method.[17]

For *in situ* FTIR analysis, samples were pressed (~1.5 tons) into self supporting discs (15 20 mg weight, 2 cm^2 area). All samples were placed in a quartz cell equipped with KBr windows. A movable quartz sample holder permits the adjustment of the pellet in the infrared beam for spectra acquisition, and to displace it into a furnace at the top of the cell for thermal treatments. The cell was connected to a vacuum line and a glass injection loop. After the activation of the sample, different probe molecules were added in small doses. For the CO adsorption experiment, the cell was cooled with liquid nitrogen. Transmission IR spectra were recorded on a Nicolet Nexus spectrometer equipped with an extended KBr beam splitting device and a mercury cadmium telluride (MCT) cryodetector. Data were collected in the 600 5600 cm^{-1} range at 4 cm^{-1} resolution with 256 scans.

Results and discussion

Non-aqueous and aqueous syntheses

The theoretic reaction path of a fluorolytic sol gel synthesis can be described by eqn (1). However, the fluorination reaction is usually incomplete, leaving residual OR groups in the obtained fluoride. The precursor $M(OR)_n$ can be alkoxide, acetate, ace tylacetonate or even inorganic salt.[18] Metal alkoxides have been frequently used in our previous studies because of their high reactivity. Consequently, working with metal alkoxides requires inert conditions to avoid side reactions. Thus we usually employ the strict Schlenk technique to handle metal alkoxides. In the search of a robust precursor for ZnF_2, we compared zinc alkoxides and acetate. Zinc acetate is finally preferred, thanks to its facile accessibility, low price and easy handling.

$$M(OR)_n + nHF \rightarrow MF_n + nROH \quad (1)$$

Moreover using zinc acetate as a precursor would allow us to perform the synthesis in an aqueous environment, because zinc acetate, unlike alkoxide, does not hydrolyse severely in the presence of water. We calculated the assumed chemical compo sitions of the ZnF_2 samples from elemental analysis results, noticing that fluorine contents of the aqueous series (ZnF_2 100 40) are slightly higher than that of *HS* ZnF_2 (Table 1, column 4). ZnF_2 100 was synthesised in a system with limited water content, which mainly came from an undehydrated precursor and solvent, and from the contact with air. In contrast, *HS* ZnF_2 was syn thesised under strictly water free conditions. The higher fluorine content suggests that the presence of water in the synthesis system environment might have a positive effect on the

Table 1 Results of elemental analysis of zinc fluoride samples

Sample name	Element (wt%)			Calculated composition[a]
	C	H	F	
HS ZnF_2	5.4	0.9	29.4	$ZnF_{1.76}(CH_3COO)_{0.24}(CH_3OH)_{0.04}$
ZnF_2 100	4.6	0.8	33.1	$ZnF_{1.84}(CH_3COO)_{0.16}(CH_3OH)_{0.08}(H_2O)_{0.01}$
ZnF_2 71	2.7	0.6	34.6	$ZnF_{1.92}(CH_3COO)_{0.08}(CH_3OH)_{0.08}(H_2O)_{0.04}$
ZnF_2 40	2.9	0.6	32.3	$ZnF_{1.88}(CH_3COO)_{0.12}(CH_3OH)_{0.02}(H_2O)_{0.10}$

[a] Theoretical elemental contents: ZnF_2: F 36.9%; $ZnF_{1.76}(CH_3COO)_{0.24}(CH_3OH)_{0.04}$: C 5.5%, H 0.8%, F 29.4%; $ZnF_{1.84}(CH_3COO)_{0.16}(CH_3OH)_{0.08}(H_2O)_{0.01}$: C 4.2%, H 0.7%, F 30.8%; $ZnF_{1.92}(CH_3COO)_{0.08}(CH_3OH)_{0.08}(H_2O)_{0.04}$: C 2.6%, H 0.6%, F 33.3%; $ZnF_{1.88}(CH_3COO)_{0.12}(CH_3OH)_{0.02}(H_2O)_{0.10}$: C 2.8%, H 0.6%, F 32.4%.

fluorination degree. A similar effect was already observed for other fluorides.[9,19]

Fundamental properties of nanoscopic ZnF_2

The sol gel prepared ZnF_2 is a novel material; we expected it would exhibit different properties as compared to the conven tional crystalline phase and determined them. First of all we performed DLS measurements to determine the ZnF_2 sol particle size distribution. The hydrodynamic radius of the sol particle follows approximately a log normal distribution with the mean at *ca.* 8 nm (Fig. 1), corresponding to an estimated average diameter of *ca.* 16 nm. The small sol particle size helps us to understand the broad reflections in XRD patterns (Fig. 3) and confirms that the obtained ZnF_2 is nanoscopic.

After evaporation of the solvent in sols and further calcina tion, we obtained powder like ZnF_2 samples. We investigated the thermal behaviour of ZnF_2 samples by DTA TG MS measure ments. The DTA TG curves and MS profiles of ZnF_2 100 are shown in Fig. 2. The other samples exhibited similar behaviours; therefore we limit the discussion to one representative example. ZnF_2 100 underwent a stepwise decomposition during the heat ing run. The weight loss of the first stage is mainly due to the release of water (m/z = 18) and methanol (m/z = 31), which is accompanied by a very broad endothermal peak between 120 and 250 °C. The DTA curve features another broad endothermal peak between 250 and 380 °C, which can be attributed to the decomposition and release of remaining acetate groups (m/z = 44 and 60). Release of HF (m/z = 19) was not observed, indicating that ZnF_2 is thermally stable.

Another fundamental property of every fluorolytic sol gel prepared metal fluoride is the low crystallinity degree, which reflects disordering in the structure or the possible existence of

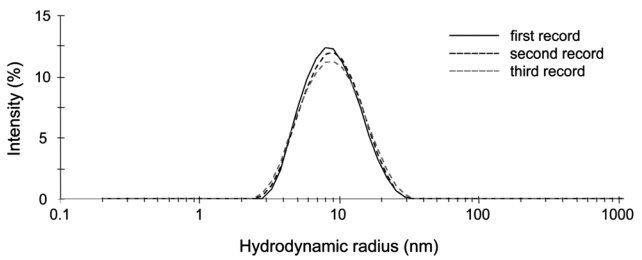

Fig. 1 ZnF_2 100 sol particle size distributions by intensity; the measurement was recorded three times and the results are reproducible.

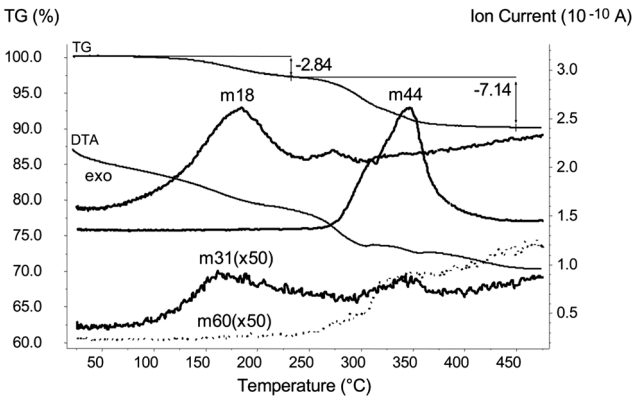

Fig. 2 DTA TG curves and MS profiles of ZnF_2 100.

nanoparticles. Structural information of ZnF_2 was obtained by powder XRD and solid state MAS NMR spectroscopy. Commercial ZnF_2 (Aldrich, 99%) was measured as a reference. Like other reported *HS* metal fluorides,[1,20,21] *HS* ZnF_2 is highly disordered, thus exhibiting only broad reflections, which indi cates its nanoscopic nature. No significant difference was found between *HS* ZnF_2 (Fig. 3a) and ZnF_2 100 (Fig. 3b). This suggests that trace amounts of water in the solvent and atmo sphere during the synthesis of ZnF_2 100 have no measurable effects on the crystallisation. However, as water content increases in the synthesis process, crystallisation becomes more distinct, which might be associated with the higher fluorination degree of these samples (Fig. 3c and d and Table 1).

Fig. 4 shows the ^{19}F MAS NMR spectra of *HS* ZnF_2 and ZnF_2 100. In the crystal structure of anhydrous zinc acetate, Zn is tetrahedrally coordinated.[22] In crystalline ZnF_2, however, the Zn centre is octahedrally coordinated by six crystallographically equivalent F. By adding HF to zinc acetate, F substitutes $OOCCH_3$ groups and forms ZnF_6 octahedra. Accordingly, the spectrum of commercial ZnF_2 displays only one symmetric signal. The main signals of the *HS* ZnF_2 and ZnF_2 100 samples are almost identical to that of the commercial ZnF_2, suggesting that the dominating fluorine species remains the same. There is an asymmetric shoulder with the chemical shift of *ca.* 195 ppm at the low field part of both spectra, which indicates the existence of fluorine in other coordination types. This is probably caused by the residual acetate groups, which result in partially fluori nated $ZnF_{6-x}O_x$ units. A similar asymmetric shoulder in the low filed part of the ^{19}F MAS NMR spectra was observed for the

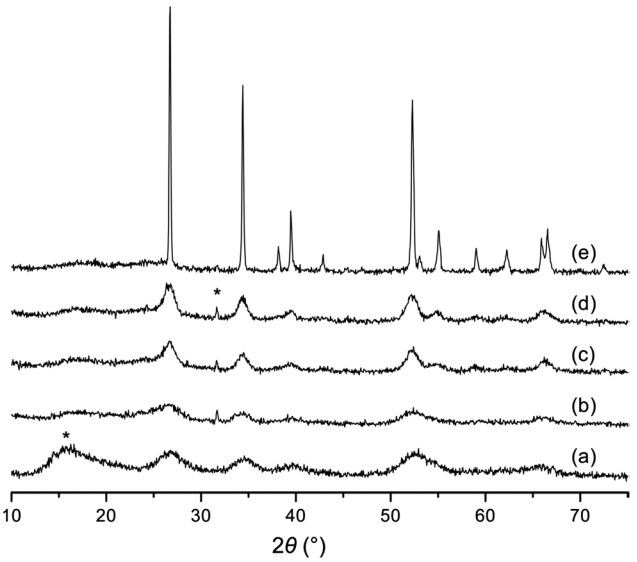

Fig. 3 XRD patterns of (a) *HS* ZnF_2, (b) ZnF_2 100, (c) ZnF_2 70, (d) ZnF_2 40 and (e) commercial ZnF_2; reflections from the sample holder are marked with *.

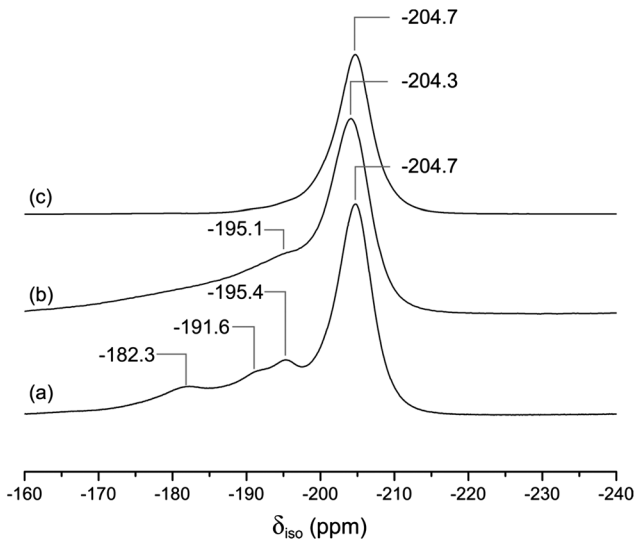

Fig. 4 ^{19}F MAS NMR spectra of (a) ZnF_2 100, (b) *HS* ZnF_2 and (c) commercial ZnF_2; positions of the main signal and shoulder peaks are indicated in the spectra.

crystal structure of $[Mg_6(\mu_4\ F)_2(\mu_3\ OMe)_4(MeOH)_{12}]$ [23,24] as well as for different hydroxylated magnesium fluorides.[19] The increase in the amount of hydroxyl groups, and hence the increasing amount of $MgF_{6-x}O_x$ units, was reflected in the appearance of a low field shift in the ^{19}F spectra as it is also observed for the ZnF_2 100 sample with two more shoulders at 191.6 and 182.3 ppm.

An astonishing high surface area is characteristic for sol gel prepared metal fluorides. Therefore these samples were given the series name "*HS* MF_n". We expected ZnF_2 should be of no exception as well. To validate this assumption, the surface area of sol gel synthesised ZnF_2 was characterised by N_2 adsorption desorption measurements at 196 °C (Table 2). Compared to

Table 2 Surface area and textural properties of zinc fluoride samples

Sample name	BET surface area ($m^2\ g^{-1}$)	Total pore volume ($cm^3\ g^{-1}$)	Average pore size diameter (nm)
HS ZnF_2	140	0.08	3
ZnF_2 100	110	0.14	5
ZnF_2 71	100	0.14	6
ZnF_2 40	90	0.14	7
Commercial ZnF_2	<10	0.01	63

commercial ZnF_2 (S.A. < 10 $m^2\ g^{-1}$), all the sol gel synthesised ZnF_2 samples had a significantly larger surface area (S.A. = 90 140 $m^2\ g^{-1}$). Nevertheless, the specific surface area of the ZnF_2 100 40 samples was smaller than that of *HS* ZnF_2, which can be connected to the higher crystallinity of these samples as suggested by XRD patterns. The adsorption desorption isotherms of *HS* ZnF_2 and ZnF_2 100 are presented in Fig. 5. Small mesopores (3 5 nm) in both samples are confirmed by a closing of the hysteresis loop (type IV isotherm plot) at the p/p_0 value of *ca.* 0.4.[25,26]

Study of surface acid base properties of ZnF_2

Our primary concern is the surface acid base properties of ZnF_2, because they highly influence the potential of ZnF_2 as a heterogeneous catalyst. To this end, *in situ* FTIR spectroscopy with probe molecules is a powerful technique, as it is able to detect surface species at the molecular level. The high sensitivity of this technique has been already demonstrated.[27] Our aim was to use this technique with different probe molecules for the characterisation of the acidity as well as the basicity of sol gel prepared ZnF_2.

For each adsorption experiment the ZnF_2 100 sample was evacuated at 200 °C for 12 h to eliminate surface impurities. Fig. 6A displays the resulting IR spectrum. The residual acetate like species are well characterised by bands at 1563 and 1456 cm^{-1}. The occurrence of a weak band at 1640 cm^{-1} indicates the presence of a small amount of adsorbed water. However, this

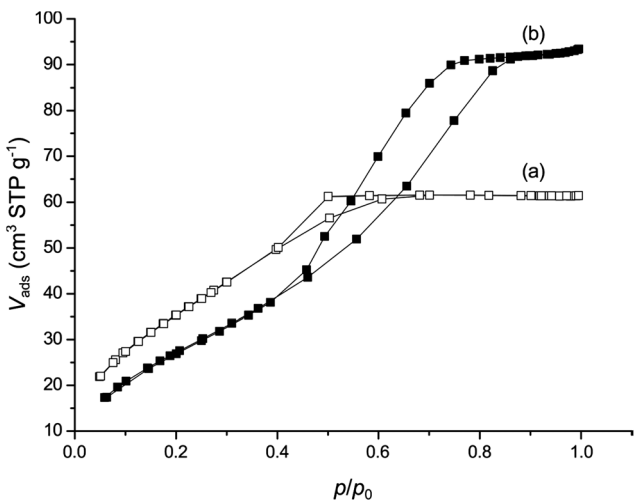

Fig. 5 N_2 adsorption desorption isotherms of (a) *HS* ZnF_2 and (b) ZnF_2 100.

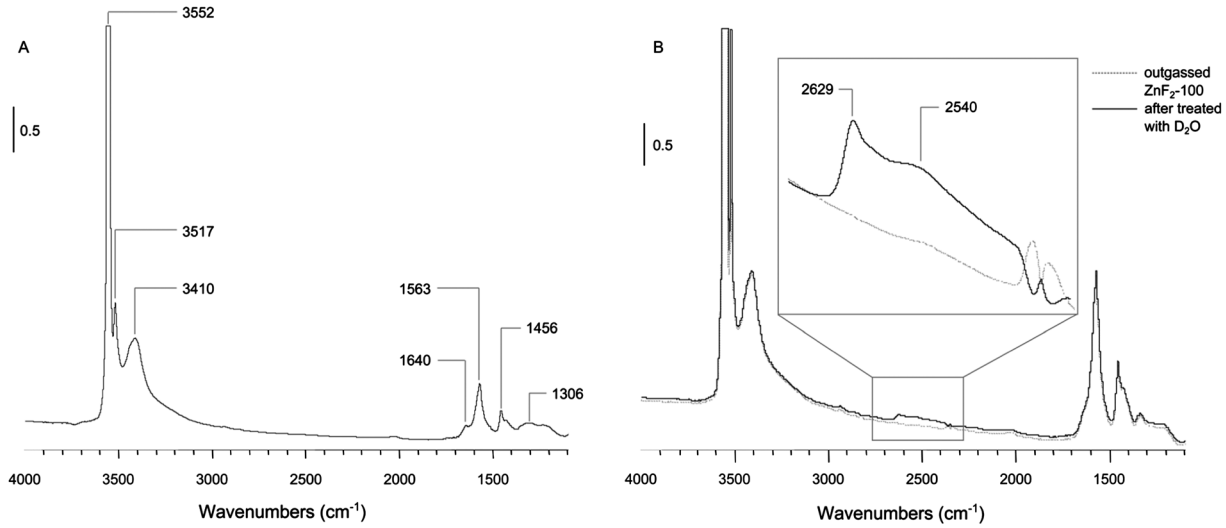

Fig. 6 (A): IR spectrum of ZnF_2 100 outgassed at 200 °C and (B): IR spectrum of outgassed ZnF_2 100 after treated with D_2O (10 Torr at equilibrium pressure and then outgassed at 200 °C).

weak peak cannot explain the high intensity of the strong ν(OH) bands at 3552, 3517 and 3410 cm ^{1} (broad). Therefore, we conclude the existence of Zn OH bindings. The assignment of these species is not straightforward, since previous studies reported the presence of OH groups on zinc oxide at 3670, 3625 and 3445 cm ^{1}.[28] Recently, a FTIR investigation performed under UHV conditions combining single crystal HREELS results showed that OH groups formed on defects exhibit IR bands at 3564 and 3448 cm ^{1}, which is closer to our positions. Moreover, the presence of fluorine in the present samples is supposed to enhance the acidity of the hydroxyls,[29] thus lowering their spec tral positions. In order to determine the location of OH groups, H/D exchange experiments with D_2O have been performed at 100 °C (Fig. 6B). Two very weak ν(OD) bands are detected at 2629 and 2540 cm ^{1}, showing that Zn OH groups are not accessible to D_2O and hence are located in the bulk. This location is confirmed by the following infrared experiments performed with different probe molecules, since no ν(OH) band perturba tion has been observed whatever the probe used.

In order to investigate two important associated properties, *i.e.* acidity and basicity, we designed three complementary experi ments by using *in situ* FTIR with different probe molecules: CO for acid sites, pyrrole for base sites, and finally $CHCl_3$ for the characterisation of the acid base pairs.

CO is known as a convenient probe molecule for detecting surface acidity. The frequency of the stretching vibration of the CO molecule is sensitive to the strength of the acid sites.[30] Progressive adsorption of small doses of CO at 173 °C on activated ZnF_2 gave rise to four distinct ν(CO) bands (Fig. 7A), those of higher wavenumber appearing first. The band at 2142 2140 cm ^{1} is typical for weak and unspecifically physisorbed CO. The other bands are assigned to linear adsorption of CO onto different coordinatively unsaturated Zn^{2+} sites. Earlier studies of CO adsorbed onto ZnO[31,32] assigned two main bands in similar positions to carbonyls adsorbed onto different crystal planes, which are in nature also unsaturated cationic sites. However, we cannot take the CO adsorption bands on ZnO as references because ZnF_2 and ZnO are structurally different. Therefore, the assignments of the different main bands were done by referencing the results of CO adsorbed onto the structurally similar, sol gel prepared MgF_2.[33] The band with the highest shift at 2197 2185 cm ^{1} is assigned to 3 fold Zn^{2+} sites (3 fold Mg^{2+}: 2201 2189 cm ^{1}); the band at 2180 2172 cm ^{1} to 4 fold Zn^{2+} sites (4 fold Mg^{2+}: 2187 2181 cm ^{1}), and the band at 2158 2153 cm ^{1} to 5 fold Zn^{2+} sites (5 fold Mg^{2+}: 2168 cm ^{1}), respectively (Fig. 7B). A comparison with MgF_2 reveals that the ν(CO) bands for ZnF_2 are situated at lower wavenumbers, indicating that the Lewis acid strength is lower on ZnF_2 for the equivalent sites. Because Zn (χ = 1.65) is more electronegative than Mg (χ = 1.31),[15] the resulting Zn F is less polar, which leads to the higher e density at Zn^{2+} (as compared to Mg^{2+}). As a result, the Lewis acidity is weaker at Zn^{2+} sites.

Elucidation of the strength of Lewis basicity is an important issue for the later understanding of the catalytic behaviour as well.[16] For this purpose pyrrole is a suitable probe molecule because it is an H bond donating molecule and can form H bound species.[34] Moreover, the applicability of this probe molecule for measuring the basic strength of fluorides was already demonstrated.[16,33] The spectra were recorded after introducing an excess of pyrrole at room temperature, fol lowed by outgassing the sample for 1 min with primary vacuum and afterwards with secondary vacuum. One broad band is identified between 3450 and 3350 cm ^{1} (Fig. 8A), which is similar to our observation from the spectrum of liquid pyrrole. Its intensity decreases after evacuation at room temperature, showing a shoulder at about 3320 cm ^{1}, due to the H bonded species with surface fluorine atoms (Fig. 8B). The red shift of the N H stretching frequency is not very high ($\Delta\nu$(NH) = 177 cm ^{1}) with respect to that of the gas phase (ν_{gas} = 3497 cm ^{1}). The result shows the presence of a small number of basic sites, weaker than those found on the sol gel prepared MgF_2, which are characterised by a ν(NH) band at 3270 cm ^{1} ($\Delta\nu$(NH) = 227 cm ^{1}).[33] This is in coincidence with the electronegativity order, because the less electronegative Mg results in more polar bonds and thus a more electron saturated F in MgF_2.

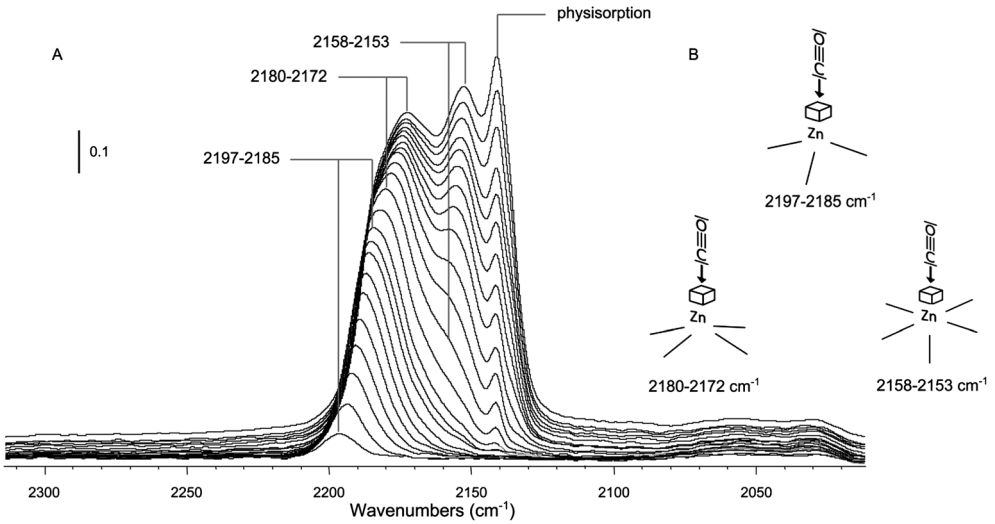

Fig. 7 (A): Differential IR spectra of CO adsorbed onto ZnF_2 100 outgassed at 200 °C and after adding successive doses of CO at 173 °C and finally 1 Torr of CO at equilibrium pressure and (B): assignments of the CO wavenumbers (in cm ^{1}) of coordinated CO on 3 , 4 and 5 fold coordinated Zn sites.

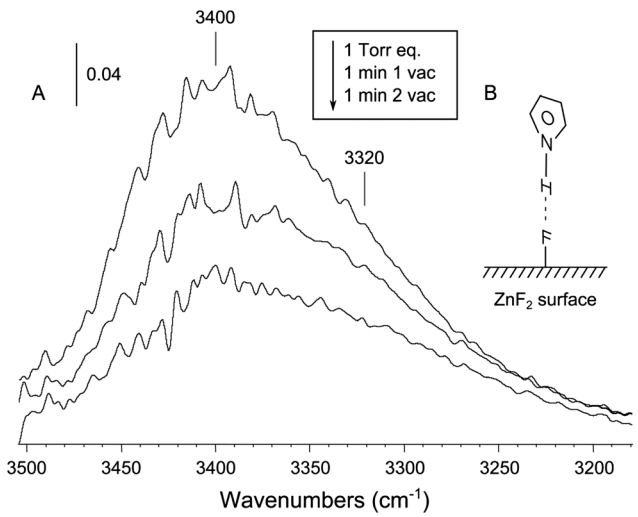

Fig. 8 (A): Differential IR spectra of pyrrole adsorbed onto ZnF_2 100 outgassed at 200 °C after adding 1 Torr of pyrrole and then outgassed under primary vacuum (1 min and 5 min, respectively) and (B): schematic illustration of the main interaction of pyrrole with the ZnF_2 surface.

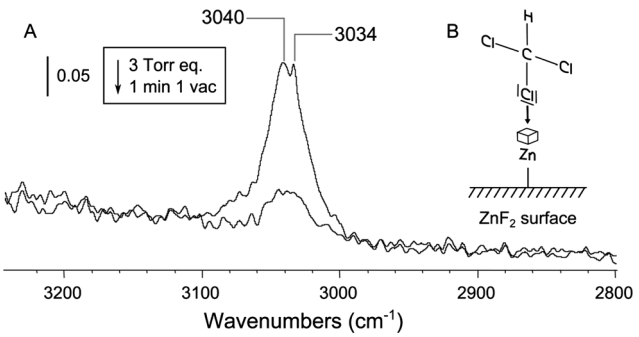

Fig. 9 (A): Differential IR spectra of adsorbed $CHCl_3$ onto ZnF_2 100 outgassed at 200 °C after injecting 3 Torr of $CHCl_3$ at equilibrium pressure followed by 1 min evacuation under primary vacuum and (B): schematic illustration of the main interaction of $CHCl_3$ with the ZnF_2 surface.

After investigating the acid sites and base sites separately, we were interested in a study of the acid base pairs. $CHCl_3$ was used as the probe molecule for this purpose because it can interact with both sites contemporaneously.[34,35] Fig. 9A presents the spectra of ZnF_2 100 recorded after the introduction of 3 Torr of $CHCl_3$ at equilibrium pressure followed by outgassing the sample for 1 min with primary vacuum. The persistence of a ν(CH) band near 3040 cm ^{1} evidences the formation of chem isorbed species. Its high wavenumber shows an interaction of Lewis sites with the lone pair of the chlorine atom (Fig. 9B),[35] leading to a ν(CH) band upper shift for the $CHCl_3$ molecule (ν_{gas} = 3019 cm ^{1}). No ν(CH) bands below 3010 cm ^{1} were detected indicating that the H bond acceptor interaction with fluorine is not predominant. Consequently, the acidity is overwhelming in the acid base pairs of the sol gel prepared ZnF_2.

The results of the three complementary experiments fully supported our expectations on ZnF_2: the sol gel prepared ZnF_2 is predominantly a Lewis acid solid with some weak Lewis base sites. The acidity as well as the basicity of ZnF_2 are weaker in comparison to those of the sol gel prepared MgF_2. This outcome agrees with the electronegativity order of the metals.

Conclusions

In this paper, we report for the first time the fluorolytic sol gel synthesis and characterisation of ZnF_2. We tested different synthesis parameters and found that nanocrystalline ZnF_2 with a high surface area was obtained regardless of the conditions. More importantly, we experimentally determined the surface acidity basicity of nanoscopic ZnF_2. Both Lewis acid and base sites were detected, although acidity is dominating on the surface of ZnF_2. By taking MgF_2 synthesised *via* the same route as the reference, we found that ZnF_2 is weaker in both acidity and basicity. The electronegativity order may offer an explanation for this observation, since Zn is more electronegative than Mg. This has been the first FTIR study of the sol gel prepared ZnF_2 and it paves the way towards further applications.

The sol gel synthesis and characterisation of ZnF_2 can be viewed as a pilot study in a new field of material chemistry. It suggests that metal fluorides can be of great interest with respect to their physicochemical properties. Therefore we sincerely hope that our study will contribute to the synthesis, understanding and application of further nanoscopic metal fluorides.

Acknowledgements

We thank Johannes Noack and Matthias Karg for the DLS measurements, Gudrun Scholz and Detlef Heidemann for the solid state MAS NMR measurements, and Micheal Feist for the thermal analysis. Ying Guo thanks the support from Chinese Scholarship Council (CSC). Stefan Wuttke acknowledges the Alexander von Humboldt foundation for a fellowship.

Notes and references

1 E. Kemnitz, U. Groß, S. Rudiger and C. S. Shekar, *Angew. Chem., Int. Ed.*, 2003, **42**, 4251 4254.
2 S. Rudiger and E. Kemnitz, *Dalton Trans.*, 2008, 1117 1127.
3 H. Kruger, A. Hertwig, U. Beck and E. Kemnitz, *Thin Solid Films*, 2010, **518**, 6080 6086.
4 J. Noack, L. Schmidt, H. J. Glasel, M. Bauer and E. Kemnitz, *Nanoscale*, 2011, **3**, 4774 4779.
5 S. Wuttke, S. M. Coman, J. Krohnert, F. C. Jentoft and E. Kemnitz, *Catal. Today*, 2010, **152**, 2 10.
6 B. M. Weckhuysen, *Angew. Chem., Int. Ed.*, 2009, **48**, 4910 4943.
7 G. A. Somorjai and J. Y. Park, *Angew. Chem., Int. Ed.*, 2008, **47**, 9212 9228.
8 N. Candu, S. Wuttke, E. Kemnitz, S. M. Coman and V. I. Parvulescu, *Appl. Catal., A*, 2011, **391**, 169 174.
9 S. M. Coman, S. Wuttke, A. Vimont, M. Daturi and E. Kemnitz, *Adv. Synth. Catal.*, 2008, **350**, 2517 2524.
10 S. M. Coman, V. I. Parvulescu, S. Wuttke and E. Kemnitz, *ChemCatChem*, 2010, **2**, 92 97.
11 A. Negoi, S. Wuttke, E. Kemnitz, D. Macovei, V. I. Parvulescu, C. M. Teodorescu and S. M. Coman, *Angew. Chem., Int. Ed.*, 2010, **49**, 8134 8138.
12 S. M. Coman, P. Patil, S. Wuttke and E. Kemnitz, *Chem. Commun.*, 2009, 460 462.
13 S. B. Troncea, S. Wuttke, E. Kemnitz, S. M. Coman and V. I. Parvulescu, *Appl. Catal., B*, 2011, **107**, 260 267.
14 E. Kemnitz, S. Wuttke and S. M. Coman, *Eur. J. Inorg. Chem.*, 2011, 4773 4794.
15 D. R. Lide, *Handbook of Chemistry and Physics*, CRC Press, 2003 2004.
16 K. Teinz, S. Wuttke, F. Borno, J. Eicher and E. Kemnitz, *J. Catal.*, 2011, **282**, 175 182.
17 J. M. Thomas and R. M. Lambert, *Characterisation of Catalysts*, John Wiley, Chichester, 1980.
18 J. Livage, C. Sanchez, M. Henry and S. Doeuff, *Solid State Ionics*, 1989, **32 33**(Part 2), 633 638.
19 S. Wuttke, S. M. Coman, G. Scholz, H. Kirmse, A. Vimont, M. Daturi, S. L. M. Schroeder and E. Kemnitz, *Chem. Eur. J.*, 2008, **14**, 11488 11499.
20 J. K. Murthy, U. Groß, S. Rudiger, E. Kemnitz and J. M. Winfield, *J. Solid State Chem.*, 2006, **179**, 739 746.
21 S. Wuttke, G. Scholz, S. Rudiger and E. Kemnitz, *J. Mater. Chem.*, 2007, **17**, 4980 4988.
22 W. Clegg, I. R. Little and B. P. Straughan, *Acta Crystallogr.*, 1986, **42**, 1701 1703.
23 A. Dimitrov, S. Wuttke, S. Troyanov and E. Kemnitz, *Angew. Chem., Int. Ed.*, 2008, **47**, 190 192.
24 S. Wuttke, A. Lehmann, G. Scholz, M. Feist, A. Dimitrov, S. I. Troyanov and E. Kemnitz, *Dalton Trans.*, 2009, 4729 4734.
25 G. Leofanti, M. Padovan, G. Tozzola and B. Venturelli, *Catal. Today*, 1998, **41**, 207 219.
26 S. Brunauer, L. S. Deming, W. E. Deming and E. Teller, *J. Am. Chem. Soc.*, 1940, **62**, 1723 1732.
27 A. Vimont, F. Thibault Starzyk and M. Daturi, *Chem. Soc. Rev.*, 2010, **39**, 4928 4950.
28 G. Ghiotti, F. Boccuzzi and R. Scala, *J. Catal.*, 1985, **92**, 79 97.
29 A. Vimont, M. Daturi and J. M. Winfield, *Functionalized Inorganic Fluorides: Synthesis, Characterizations & Properties of Nanostructured Solids*, Wiley Blackwell, 2010.
30 J. A. Lercher, C. Grundling and G. Eder Mirth, *Catal. Today*, 1996, **27**, 353 376.
31 K. I. Hadjiivanov and G. N. Vayssilov, in *Advances in Catalysis*, Academic Press, 2002, pp. 307 511.
32 J. C. Lavalley, J. Saussey and A. A. Tsyganenko, *Surf. Sci.*, 1994, **315**, 112 118.
33 S. Wuttke, A. Vimont, J. C. Lavalley, M. Daturi and E. Kemnitz, *J. Phys. Chem. C*, 2010, **114**, 5113 5120.
34 J. C. Lavalley, *Catal. Today*, 1996, **27**, 377 401.
35 S. Huber and H. Knozinger, *J. Mol. Catal. A: Chem.*, 1999, **141**, 117 127.